

Effects of Shearing Flow with Inertia on Monolayer Mesoscale Structure

Amir H. Hirsaa,*[†] Juan M. Lopez,[‡] Michael J. Vogel,[§] and Jonathan J. F. Leung[†]

Department of Mechanical, Aerospace and Nuclear Engineering, Rensselaer Polytechnic Institute, Troy, New York 12180, Department of Mathematics and Statistics, Arizona State University, Tempe, Arizona 85287, and School of Chemical and Biomolecular Engineering, Cornell University, Ithaca, New York 14853

Received July 10, 2006. In Final Form: September 8, 2006

In an experimental flow system capable of imparting a well-controlled shear-rate distribution with inertia to a monolayer consisting of coexisting phases, we have studied the resulting phase morphology and domain fragmentation. These evolve on distinct time scales: the viscous time associated with the viscosity in the bulk and the Marangoni stress and the fragmentation/relaxation time associated with the phase morphology. A relationship between the microstructure (line tension) and macroflow (shear rate) determining the meso length scale of the coexisting phase domains has been deduced from dimensional analysis and was found to correlate well with the quantitative experimental observations.

Monolayers at air/water interfaces are ubiquitous in nature and technology, and the realization of a monolayer-free air/water interface is practically impossible. Surfactant monolayers are important in life processes, including respiration.¹ Monolayer-forming surfactants are added for functionality in material (e.g., foams) and food (as emulsifiers) processing and in liquid injection and atomization systems (e.g., inkjets). Hence, there is wide interest in understanding the intrinsic physical processes associated with monolayer hydrodynamics.

The microscopic structure of monolayers and their thermodynamic state have been widely studied.^{2,3} At the other extreme, the macroscopic description of how monolayers couple to bulk hydrodynamics has also been widely studied, without accounting for the microstructure.^{4,5} This is usually done by coupling the Navier–Stokes equations for the bulk flow to a Newtonian surface model for the monolayer-covered gas/liquid interface.⁶ Departures from Newtonian behavior in monolayer hydrodynamics have typically been ascribed to nonlinearities in the stress–strain relation while maintaining the homogeneity of the film in the model. However, microscopic observations of monolayers over a wide range of conditions reveal heterogeneous structure consisting of coexisting phase domains.

In fluid monolayers consisting of two coexisting phases where one is a gas phase and the other is a liquid phase or both phases are liquid with different packing densities, most studies have considered monolayers in static equilibrium, and the response to a small deformation of a distinct domain has been qualified by measuring its relaxation.⁷ The balance between line tension and long-range forces due to dipole interactions has also been examined in quiescent systems.⁸ In the analysis of these systems,

the hydrodynamic coupling between multidomain monolayers and the liquid substrate has been neglected. However, when the system is driven away from equilibrium into the fully nonlinear regime, this coupling cannot be ignored.⁹ The effects of flow on these systems have typically been studied in the inertia-less limit^{10,11} or when inertia is small,^{12,13} and the reversibility typically observed in bulk Stokes flow is also seen in the monolayer with the domains relaxing to their original shape.¹⁴ A significant advance in our understanding resulted from the experiments in ref 15 where both large and small shearing deformations of domains and their subsequent relaxations gave the same estimate of line tension, suggesting that the line tension is intrinsic and not dependent on the flow.

Here we report on the response of a monolayer to strong shear in a flow with significant inertia. This leads to very large departures from circular shapes, resulting from the line tension between the two monolayer phases, into narrow and highly elongated domains aligned with the direction of shear. Dimensional analysis leads to a relationship involving the viscosity of the substrate, the strain rate at the surface, the line tension between the monolayer phase domains, and the length scale of the deformed domains. We have made direct experimental measurements of the domains and the shear flow; these are consistent with this relationship. This result provides new insight into the hydrodynamic coupling between the microscopic behavior of the monolayer (length scales of the domains and the line tension between them) and the macroscale behavior of the flowing substrate.

We have studied this coupling in a geometrically simple setup allowing for precise, well-controlled experiments. Figure 1 shows a schematic of the flow apparatus consisting of a circular cylinder of radius $R = 2.5$ cm and height $H = 0.66$ cm, filled with water at 22.5 °C (kinematic viscosity $\nu = 0.0095$ cm²/s). The flow is driven by the constant rotation of the bottom disk at Ω rad/s. In nondimensionalized terms, this is the Reynolds number $Re =$

* Corresponding author. E-mail: hirsaa@rpi.edu.

[†] Rensselaer Polytechnic Institute.

[‡] Arizona State University.

[§] Cornell University.

(1) Grothberg, J. B. *Annu. Rev. Fluid Mech.* **1994**, *26*, 529–571.

(2) Knobler, C. M.; Desai, R. C. *Annu. Rev. Phys. Chem.* **1992**, *43*, 207.

(3) Kaganer, V. M.; Möhwald, H.; Dutta, P. *Rev. Mod. Phys.* **1999**, *71*, 779–819.

(4) Slattery, J. C. *Interfacial Transport Phenomena*; Springer: New York, 1990.

(5) Edwards, D. A.; Brenner, H.; Wasan, D. T. *Interfacial Transport Processes and Rheology*; Butterworth-Heinemann: Boston, 1991.

(6) Scriven, L. E. *Chem. Eng. Sci.* **1960**, *12*, 98–108.

(7) McConnell, H. M. *Annu. Rev. Phys. Chem.* **1991**, *42*, 171–195.

(8) de Koker, R.; McConnell, H. M. *J. Phys. Chem.* **1993**, *97*, 13419–13424.

(9) Gallez, D.; McConnell, H. M. *J. Phys. Chem. B* **2000**, *104*, 1657–1662.

(10) Benvegnu, D. J.; McConnell, H. M. *J. Phys. Chem.* **1992**, *96*, 6820–6824.

(11) In the inertia-less limit, the nonlinear advection terms are negligible in comparison to the linear diffusive terms.

(12) Dennin, M.; Knobler, C. M. *Phys. Rev. Lett.* **1997**, *78*, 2485.

(13) Iñes-Mullol, J.; Schwartz, D. K. *Phys. Rev. Lett.* **2000**, *85*, 1476.

(14) Ivanova, A. N.; Iñes-Mullol, J.; Schwartz, D. K. *Langmuir* **2001**, *17*, 3406–3411.

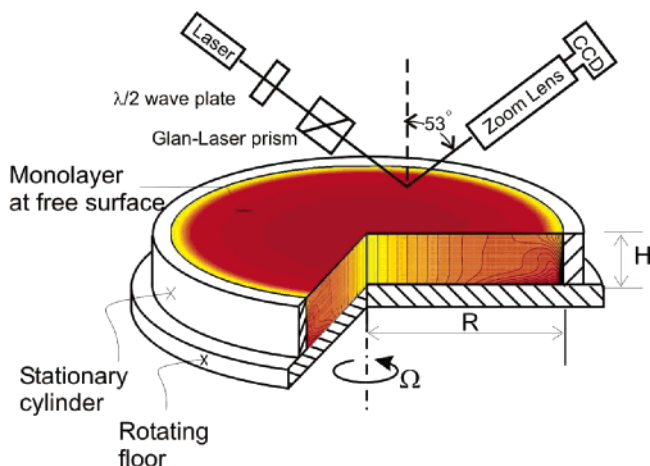


Figure 1. Schematic of the experimental setup. The inset (meridional cuts) shows the vortex lines, and the colored shading on the surface shows the monolayer concentration distribution obtained from numerical simulations. Note the nearly solid-body rotation (evenly spaced vortex lines) in the central part of the flow.

$\Omega R^2/\nu$. We drive the system with large inertia to just below the level at which the bulk flow becomes unstable to 3D perturbations. Specifically, we set $Re = 1000$ (the critical Re for $H/R = 0.25$ with a nominally clean air/water interface is about 1450), at which a wide range of shear is imposed by the axisymmetric flow across the air/water interface. The bulk flow consists of two regions: for $r \lesssim 0.5R$ it is in solid-body rotation, and for $r \gtrsim 0.5R$, it is an overturning flow advecting angular momentum from the rotating floor boundary layer up to the interface imposing a radial distribution of the azimuthal shear onto the monolayer. The cutouts in Figure 1 show the vortex lines illustrating this flow.

A monolayer of vitamin K_1 , which is well-behaved,^{16–18} is spread on the air/water interface before the bottom disk is set to rotate. The macroscopic coupling between this monolayer and the bulk is relatively simple because it involves only surface tension gradients (i.e., Marangoni stress¹⁹). There is no measurable surface shear viscosity for the range of monolayer concentrations encountered, and the steady flow is not sensitive to surface dilatational viscosity. Furthermore, vitamin K_1 monolayers have domains that are clearly visualized using BAM (Brewster angle microscopy). The technical details of this flow system are presented in refs 20 and 21. The details of the BAM system are given in refs 22 and 23, and details of the macroscopic behavior of vitamin K_1 on flowing systems are given in refs 24–26.

(15) Lauger, J.; Robertson, C. R.; Frank, C. W.; Fuller, G. G. *Langmuir* **1996**, *12*, 5630–5635.

(16) Vitamin K_1 monolayers are well behaved in that measurements of the equation of state obtained through the standard technique of surface compression in a Langmuir trough give essentially identical results to measurements conducted during surface expansion over a wide range of initial and final monolayer surface concentrations.

(17) Weitzel, G.; Fretzdorff, A.-M.; Heller, S. *Hoppe–Seyler’s Z. Physiol. Chem.* **1956**, *303*, 14–26.

(18) Gaines, G. L. *Insoluble Monolayers at Liquid–Gas Interfaces*; Interscience: New York, 1966.

(19) The coupling between the monolayer and the superphase (air) has been shown to be negligible by comparisons between experiments and theory that ignores the coupling.

(20) Miraghaie, R.; Lopez, J. M.; Hirsra, A. H. *Phys. Fluids* **2003**, *15*, L45–L48.

(21) Lopez, J. M.; Marques, F.; Hirsra, A. H.; Miraghaie, R. *J. Fluid Mech.* **2004**, *502*, 99–126.

(22) Vogel, M. J.; Hirsra, A. H.; Miraghaie, R.; Lopez, J. M. *Langmuir* **2004**, *20*, 5651–5654.

(23) Lopez, J. M.; Vogel, M. J.; Hirsra, A. H. *Phys. Rev. E* **2004**, *70*, 056308.

(24) Hirsra, A. H.; Lopez, J. M.; Miraghaie, R. *J. Fluid Mech.* **2001**, *443*, 271–292.

(25) Hirsra, A. H.; Lopez, J. M.; Miraghaie, R. *J. Fluid Mech.* **2002**, *470*, 135–149.

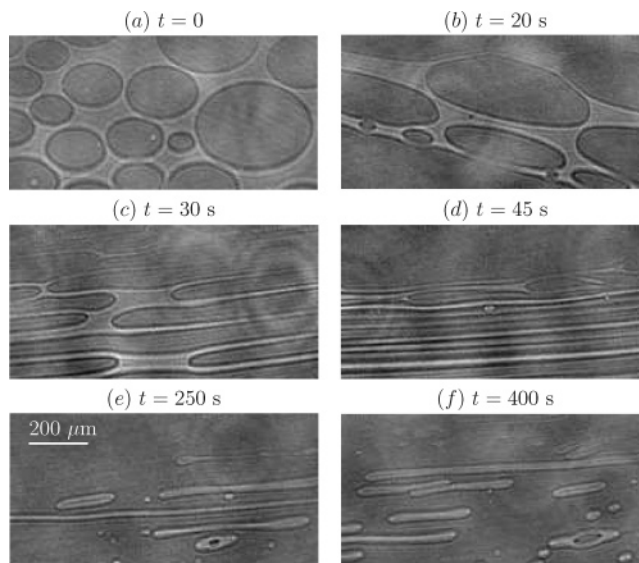


Figure 2. BAM images taken at $r = 0.7R$ of a vitamin K_1 monolayer with initial concentration $C_0 = 0.4 \text{ mg/m}^2$. At $t = 0$, the floor of the cylinder of aspect ratio $H/R = 0.265$ was impulsively started to rotate from rest to a nondimensional rotation rate $Re = 1000$. Images at subsequent times as indicated are shown. The axis of rotation is toward the top of the page.

The vitamin K_1 monolayer reaches static equilibrium on the surface of water after a period of about 10 to 15 min following the spreading and evaporation of the solvent (high-purity hexane). For a range of monolayer concentrations, the monolayer on quiescent water consists of a dispersed phase with a relatively low packing density (liquid-expanded phase that appears as dark regions in BAM images) surrounded by a continuous phase with high packing density (liquid-condensed phase with a brighter appearance in BAM images). Figure 2a shows a BAM image for a monolayer (average) concentration of $C_0 = 0.4 \text{ mg/m}^2$ immediately before the floor was set in motion ($t = 0$). The domains are circular as a consequence of the line tension between the two phases and the apparent lack of other effects such as polarity.⁷ (They are oval in the photographs because of the BAM angle of view.) The sequence of BAM images shown in Figure 2 was taken at a fixed location ($r = 0.7R$) at various times following the impulsive start of the floor rotation at $t = 0$. Numerical solutions of the Navier–Stokes equations with a Newtonian surface model for the monolayer show that steady state is reached in about 40 s, which is approximately the viscous time H^2/ν . Figure 2d shows that at $t = 45 \text{ s}$ the now steady macroscopic bulk flow has stretched the coexisting monolayer phase domains such that the bright regions (liquid-condensed phase) are elongated into very thin strips aligned with the shear. Figure 2e and f shows that the monolayer phase domains continue to evolve via fragmentation into progressively smaller domains. Nevertheless, their widths appear to remain constant by the time the bulk flow reaches steady state ($\sim 40 \text{ s}$). At other radial locations on the interface, where the shear rate is very different, the widths of the domains are different, as illustrated below. That the widths of the domains remain constant as soon as the bulk flow reaches a steady state suggests that the domain width is set by the line tension as its effect competes with the azimuthal shear at the interface. The fact that domains continue to fragment for a period of time at least 1 order of magnitude longer than the time it takes the bulk flow to develop suggests that the monolayer relaxation

(26) Vogel, M. J.; Hirsra, A. H. *J. Fluid Mech.* **2002**, *472*, 283–305.

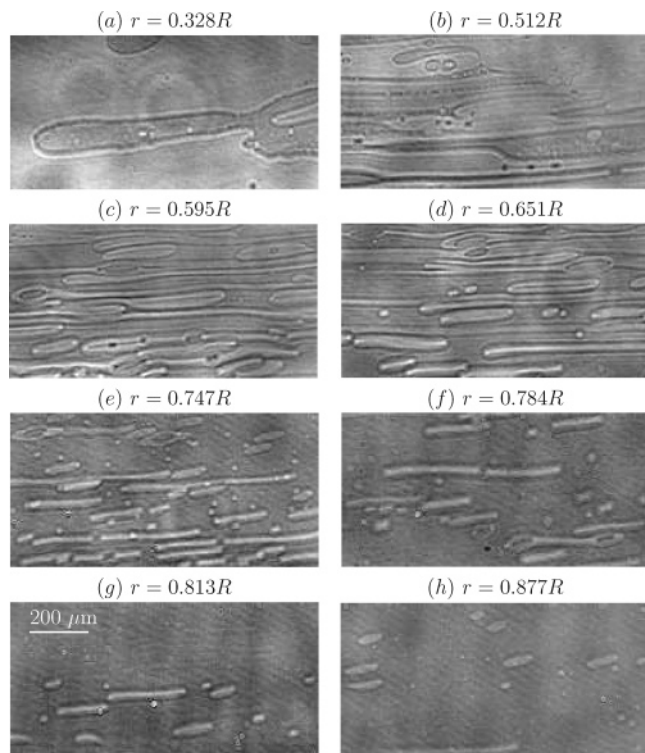


Figure 3. Radial variation of domain structures at $Re = 1000$, $H/R = 0.265$, and $C_0 = 0.4 \text{ mg/m}^2$. The eight BAM images were taken over a period of about 14 s, 600 s after the start-up of the flow. The axis of rotation is toward the top of the page.

time is independent of the flow and may be set by other intrinsic properties.

On the basis of the above results, there appear to be at least two distinct time scales governed by (i) the viscous time associated with viscosity in the bulk and the Marangoni stress responsible for setting the radial distribution of the monolayer and (ii) the fragmentation/relaxation associated with phase morphology.^{13,15,27} Others have also observed a time scale associated with the molecular polar tilt alignment with the flow direction.^{28,29}

The flow system provides a wide range of shear rates at the interface. The images presented in Figure 3 were obtained by scanning the microscope radially outward from the center about 600 s after the start of the flow. Although the eight images were acquired over a finite time (about 14 s), this is short compared to the time scale associated with monolayer fragmentation and relaxation, and thus the images may be considered to be essentially an “instantaneous” snapshot of monolayer structure following long-time exposure to various levels of azimuthal shear at the interface. In radial locations smaller than about $0.5R$, the flow is essentially in solid-body rotation,³⁰ and the low level of shear is unable to fragment the domains or even stretch them into thin regions, as shown in Figure 3a at small $r \approx 0.33R$. As the surface is scanned at larger radii, stretching of the domains associated with regions of the interface with larger shear can be seen, for example, in Figure 3b. In this region ($r \approx 0.51R$), although the

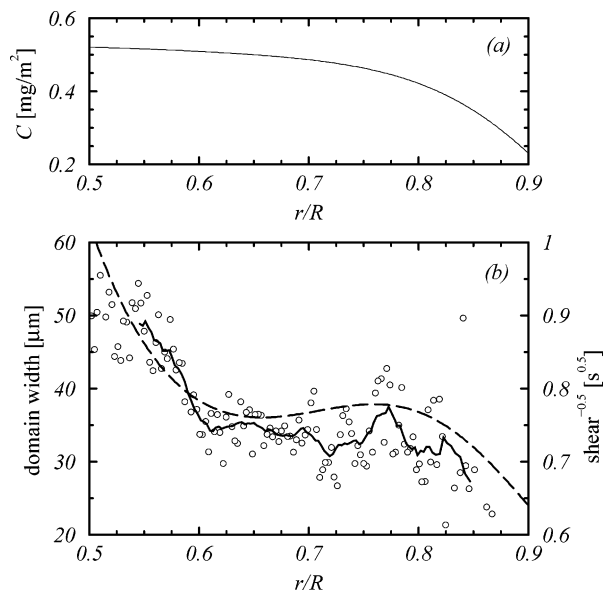


Figure 4. (a) Computed monolayer concentration profile, $C(r)$, at steady state for $Re = 1000$, $H/R = 0.25$ with $C(r) = 0.4 \text{ mg/m}^2$ at $t = 0$ and (b) the corresponding computed shear $(\dot{\gamma})^{-0.5}$ (dashed curve) and the experimentally measured width (in μm) of the domains (open symbols) and their 15-bin moving average in r (solid curve).

domains are stretched, the stress is apparently not sufficient to cause fragmentation. Figure 3 shows that a significant degree of fragmentation does not occur for $r < 0.6R$.

Aside from the large degree of fragmentation observed at large radii, Figure 3 also shows a reduction in the average coverage of the brighter (liquid-condensed) phase domains. This is attributable to the radial gradient in monolayer (average) concentration that is necessary to generate a Marangoni stress at the interface to balance the radial shear in the liquid adjacent to the interface (Figure 4a). The coupling between the bulk flow and this monolayer is relatively well understood on the macroscopic scale.^{24–26}

The present setup using a short-pulse laser for imaging the monolayer phase domains on a flowing system allows for a detailed study of how shearing of the monolayer influences the width of its coexisting phase domains. This BAM system is capable of freezing the motion of a fast-flowing monolayer, and along with the relatively high contrast between the coexisting phase domains of the vitamin K_1 monolayer, this permits a straightforward comparison between the domain width and the local surface shear rate. BAM images were obtained at a repetition rate of 15 Hz and were converted to binary images from which the domain width was determined numerically using between 10^3 and 10^4 domains. These measurements are presented in Figure 4b. A fit to these data, consisting of a 15-bin moving average, is also drawn with a solid curve to highlight the trend of the measurements. The general trend of decreasing domain width with increasing r is consistent with the larger surface shear in regions away from the solid-body rotation at the center. If we consider the shearing of an individual domain (bright region in Figure 3, for example), then the line tension is providing resistance against further narrowing of the domain width. Thus, using dimensional reasoning we find that the width of the domains W must be related to the strain rate $\dot{\gamma}$, the viscosity in the bulk $\mu = \nu\rho$, where ρ is the density, and the line tension λ as

$$W \propto \left(\frac{\lambda}{\mu \dot{\gamma}} \right)^{0.5} \quad (1)$$

(27) Maruyama, T.; Fuller, G. G.; Frank, C. W.; Robertson, C. R. *Science* **1996**, *274*, 233.

(28) Maruyama, T.; Lauger, J.; Fuller, G. G.; Frank, C. W.; Robertson, C. R. *Langmuir* **1998**, *14*, 1836–1845.

(29) Iñes-Mullol, J.; Schwartz, D. K. *Langmuir* **2001**, *17*, 3017.

(30) The inset in Figure 1 is from a Navier–Stokes computation coupled with a Boussinesq–Scriven surface model for vitamin K_1 , with $Re = 1000$ and $C_0 = 0.4 \text{ mg/m}^2$. The uniform spacing of the vortex lines up to $r \approx 0.5R$ indicates that $v \propto r$ and is therefore in solid-body rotation. In the computations reported in this letter, we use the equation of state reported in Lopez, J. M.; Hirs, A. H. *J. Colloid Interface Sci.* **2001**, *242*, 1–5.

This can be obtained formally using Buckingham's Π theorem,³¹ for example, by observing that there are four variables and parameters in this problem and three fundamental units. Thus, there is one dimensionless group governing the problem, which must be a constant. The distribution of azimuthal shear (specifically $\dot{\gamma}^{-0.5}$) across the surface obtained from the Navier–Stokes computations is plotted in Figure 4b. Although there is scatter in the measurements, the measured domain width correlates well with the computed azimuthal shear at the interface.

There have been studies in which the characteristic length scale of domains (domain radius R), viscosity of the substrate μ , and line tension between domains λ have been related to a characteristic time scale T_c for the relaxation of a slightly deformed domain back to its equilibrium state. In particular, ref 32 determined that $T_c \propto \mu R^2/\lambda$ for systems in which the substrate viscosity dominates the surface (shear) viscosity. In our experiments, the characteristic time scale corresponds to the interfacial shear rate that maintains the domains far from equilibrium ($T_c \approx 1/\dot{\gamma}$), and the characteristic length scale is the width W of the elongated domains. Our scaling relationship (eq 1) for a system maintained far from equilibrium is the same as that of ref 32 for the low-inertia relaxation back to equilibrium.

Although no data on the line tension was found in the literature for vitamin K₁, estimates of between 10^{-7} and 1.6×10^{-7} dynes for the effective line tension of other liquid-phase monolayers have been made.^{10,32,33} More recently, the effective line tension of another Langmuir monolayer (methyl octadecanoate) has been estimated to be approximately 3×10^{-6} dynes; at the temperature at which this was estimated (35 °C), this monolayer also exhibited liquid-condensed and liquid-expanded coexistence.³⁴ Of course, different monolayer systems can have a wide range of values for line tension. Coincidentally, using this value, the constant of proportionality in eq 1 happens to be of order 1.

Figure 4a shows there is a noticeable variation in the monolayer concentration over the range of $0.45R < r < 0.88R$, where the experimental data set was obtained. (BAM measurements at larger values of r suffer from significant noise due to reflections from the cylinder, and domain widths at small r approach the width of the strip imaged by BAM, making domain-width measurements unobtainable.) We have repeated the experiment with a vitamin K₁ monolayer at a much larger initial concentration, $C_0 = 0.8$ mg/m². This larger C_0 is near the upper limit for the coexistence of the liquid-condensed and liquid-expanded phases in this monolayer. However, this concentration is in the large Marangoni stress regime of the equation of state for vitamin K₁, so for the

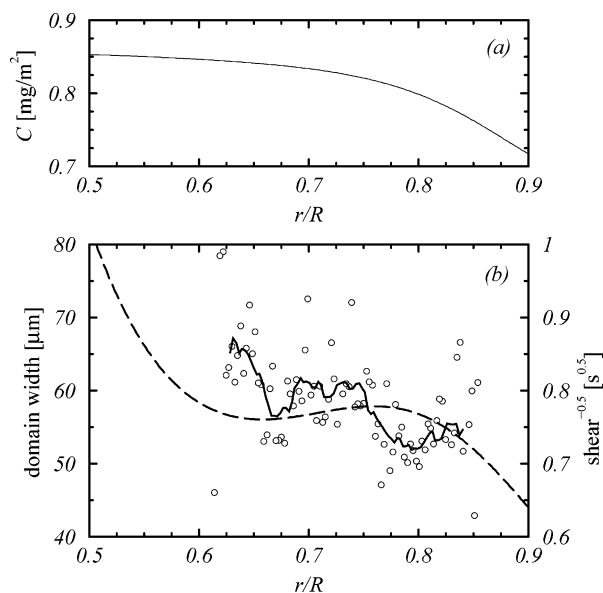


Figure 5. (a) Computed monolayer concentration profile, $C(r)$, at steady state for $Re = 1000$, $H/R = 0.25$ with $C(r) = 0.8$ mg/m² at $t = 0$ and (b) the corresponding computed shear $(\dot{\gamma})^{-0.5}$ (dashed curve) and the experimentally measured width (in μm) of the domains (open symbols) and their 15-bin moving average in r (solid curve).

same level of bulk flow inertia ($Re = 1000$), the concentration gradients are smaller than with $C_0 = 0.4$ mg/m². The concentration profile at steady state is shown in Figure 5a. Because this monolayer exhibits zero surface shear viscosity,²⁴ the surface azimuthal velocity profiles for the two C_0 values are almost identical because for both cases the interface remains completely covered by the monolayer. Hence, the corresponding shear at the surface is almost the same in both cases as well. Figure 5b shows the correlation between the domain width and $\dot{\gamma}^{-0.5}$. Although the higher C_0 data has more scatter than the lower C_0 data (Figure 4b), it also supports the scaling in eq 1. Note that the larger monolayer concentration in the $C_0 = 0.8$ mg/m² case results in larger domains, limiting the lower bound of the radial extent over which reliable BAM data could be obtained.

The widths of the (liquid-condensed) domains for the $C_0 = 0.8$ mg/m² case are about 50% larger than in the $C_0 = 0.4$ mg/m² case. This is because the ratio of liquid-condensed to liquid-expanded surface area is initially larger at larger C_0 . Because the molecular packing of each of the phases varies with the macroscopic concentration C , the line tension between the phases can also vary with C . This is an important issue that warrants further study.

Acknowledgment. This work was supported by the National Science Foundation through grants CTS0340768, CTS0340736, and DMS05052846.

LA061995N

(31) Buckingham, E. *Phys. Rev. Ser. 2* **1914**, *4*, 345–376.

(32) Mann, E. K.; Hénon, S.; Langevin, D.; Meunier, J.; Légar, L. *Phys. Rev. E* **1995**, *51*, 5708–5720.

(33) Yim, K. S.; Brooks, C. F.; Fuller, G. G.; Frank, C. W.; Robertson, C. R. Flow-Induced Deformation and Relaxation Processes of Polydomain Structures in Langmuir Monolayer. In *Organic Thin Films: Structure and Applications*; Frank, C. W., Ed.; ACS Symposium Series; American Chemical Society: Washington, DC, 1998; Vol. 695, pp 43–56.

(34) Wurlitzer, S.; Steffen, P.; Wurlitzer, M.; Khattari, Z.; Fischer, Th. M. *J. Chem. Phys.* **2000**, *113*, 3822–3828.